PLOS | ONE

RESEARCH ARTICLE

From the Ground Up: Global Nitrous Oxide Sources are Constrained by Stable Isotope Values

David M. Snider[1]*, Jason J. Venkiteswaran[2,3]*, Sherry L. Schiff[3], John Spoelstra[1,3]

1 National Water Research Institute, Canada Centre for Inland Waters, Environment Canada, Burlington, ON, L7R 4A6, Canada, **2** Department of Geography and Environmental Studies, Wilfrid Laurier University, Waterloo, ON, N2L 3C5, Canada, **3** Department of Earth and Environmental Sciences, University of Waterloo, Waterloo, ON, N2L 3G1, Canada

* dave.snider@ec.gc.ca (DMS); jvenkiteswaran@wlu.ca (JJV)

Citation: Snider DM, Venkiteswaran JJ, Schiff SL, Spoelstra J (2015) From the Ground Up: Global Nitrous Oxide Sources are Constrained by Stable Isotope Values. PLoS ONE 10(3): e0118954. doi:10.1371/journal.pone.0118954

Academic Editor: Shuijin Hu, North Carolina State University, UNITED STATES

Received: April 10, 2014

Accepted: January 8, 2015

Published: March 26, 2015

Data Availability Statement: All relevant data are within the paper and its Supporting Information files. In addition, the data and an R file that contains the code to perform the statistical analyses and create the figures shown here are found at https://github.com/jjvenky/Global-N2O-Ellipses.

Funding: This research was supported by the Natural Sciences and Engineering Research Council of Canada 'Strategic Projects' awarded to SLS: STPGP 322062-05, STPGP 365226-08, STPGP 381058-09, www.nserc-crsng.gc.ca; Natural Sciences and Engineering Research Council of Canada 'Strategic Project' co-funded by BIOCAP awarded to

Abstract

Rising concentrations of nitrous oxide (N_2O) in the atmosphere are causing widespread concern because this trace gas plays a key role in the destruction of stratospheric ozone and it is a strong greenhouse gas. The successful mitigation of N_2O emissions requires a solid understanding of the relative importance of all N_2O sources and sinks. Stable isotope ratio measurements ($\delta^{15}N$-N_2O and $\delta^{18}O$-N_2O), including the intramolecular distribution of ^{15}N (site preference), are one way to track different sources if they are isotopically distinct. 'Top-down' isotope mass-balance studies have had limited success balancing the global N_2O budget thus far because the isotopic signatures of soil, freshwater, and marine sources are poorly constrained and a comprehensive analysis of global N_2O stable isotope measurements has not been done. Here we used a robust analysis of all available *in situ* measurements to define key global N_2O sources. We showed that the marine source is isotopically distinct from soil and freshwater N_2O (the continental source). Further, the global average source (sum of all natural and anthropogenic sources) is largely controlled by soils and freshwaters. These findings substantiate past modelling studies that relied on several assumptions about the global N_2O cycle. Finally, a two-box-model and a Bayesian isotope mixing model revealed marine and continental N_2O sources have relative contributions of 24–26% and 74–76% to the total, respectively. Further, the Bayesian modeling exercise indicated the N_2O flux from freshwaters may be much larger than currently thought.

Introduction

Since the advent of the Haber-Bosch process one century ago, humans have vastly perturbed the global nitrogen (N) cycle. Current anthropogenic activities contribute 51% of the total N fixed worldwide (210 of 413 Tg N yr^{-1}) [1]. One negative consequence of this is an increase in atmospheric nitrous oxide (N_2O) [2], a long-lived trace gas that contributes to climate warming and the destruction of stratospheric ozone [3]. The current concentration of N_2O in the

SLS: STPGP 336807-06, www.nserc-crsng.gc.ca and www.biocap.ca; Natural Sciences and Engineering Research Council of Canada 'Strategic Project' awarded to JS and SLS: STPGP 357056-07, www.nserc-crsng.gc.ca; Natural Sciences and Engineering Research Council of Canada 'Discovery Grant' awarded to SLS: RGPIN 33854, www.nserc-crsng.gc.ca; Ontario Ministry of Agriculture and Food 'Environmental Sustainability Directed Research Program' projects awarded to JS: Project 09M1, Project 11M1, www.omafra.gov.on.ca; Canadian Foundation for Climate and Atmospheric Sciences project awarded to SLS: GR-428; Banting Postdoctoral Fellowship awarded to DMS, www.banting.fellowships-bourses.gc.ca; and Norfolk Land Stewardship Council project awarded to JS, www.hnstewardshipcouncils.org/norfolk_land_stewardship_council. The funders had no role in study design, data collection and analysis, decision to publish, or preparation of the manuscript.

Competing Interests: The authors have declared that no competing interests exist.

troposphere is 325 parts per billion (ppb) [4]. Future concentrations of atmospheric N_2O are difficult to predict, yet this information is an essential input parameter for global climate change models. Further, both the prediction and mitigation of N_2O concentrations depend on an accurate understanding of the emissions from key N_2O sources.

Most emissions of N_2O (natural and anthropogenic) occur from terrestrial, freshwater, and marine environments, where N compounds are processed by nitrifying and denitrifying microorganisms. These processes account for $\sim$89% of the total annual N_2O emissions, or almost 16 Teragrams (Tg = 10^{12} g) N/year [5]. However, scientists' best estimates of the N_2O budget are still highly uncertain. The most recent Intergovernmental Panel on Climate Change Assessment Report (IPCC-AR5) reveals wide ranges in the relative uncertainty of many individual N_2O sources. In addition, the uncertainty on the annual cumulative emissions of N_2O for 2006 from natural soils, oceans, rivers, estuaries, coastal zones, and agriculture combined ranged between 6.9–26.1 Tg N [5].

The clear separation and accounting of individual N_2O sources remains challenging, but is essential if we are to make meaningful reductions in emissions. Measurements of stable isotope ratios ($\delta^{15}N$-N_2O and $\delta^{18}O$-N_2O) and the intramolecular site preference (SP) of ^{15}N are one way to track sources *if* they are isotopically distinct. Several accounts of the global N_2O budget have used 'top-down' isotope mass-balance models to estimate the strength and isotopic composition of anthropogenic and natural N_2O sources [2,6–11]. In this approach, changes in atmospheric N_2O over time are modelled by comparing our modern-day atmosphere (a mixture of post-industrial, anthropogenic N_2O and natural N_2O) to relic air trapped in glacial firn and ice. All these studies have assumed that soils are the main source of post-industrial N_2O because its calculated isotopic composition was most similar to a limited body of published soil N_2O measurements. Yet we do not have a clear synthesis of the isotopic character of individual N_2O sources. For example, freshwaters and estuaries may contribute up to 25% of anthropogenic N_2O emissions [5], but prior to 2009 there was only one publication reporting freshwater $\delta^{15}N$-N_2O and $\delta^{18}O$-N_2O values [12] (S1 Dataset). In reality, there is extreme variation in the measured values of $\delta^{15}N$-N_2O and $\delta^{18}O$-N_2O (Fig. 1), and no systematic examination of individual sources has occurred.

In this paper, we use a 'bottom-up' approach to define key N_2O sources and demonstrate that their global average $\delta^{15}N$ and $\delta^{18}O$ values are isotopically unique. Further we use these *in situ* N_2O isotope data to substantiate what 'top-down' global atmospheric models have predicted; soils, and not marine or freshwater ecosystems, are the main source of rising atmospheric N_2O levels.

Methods

We mined 1920 data points from 52 studies that measured *in situ* $\delta^{15}N$-N_2O and $\delta^{18}O$-N_2O in atmospheric, terrestrial and marine systems from 1987 to present [2,10–60]. If the published data was not tabulated, we used the software 'g3data' (*http://www.frantz.fi/software/g3data.php*) to extract data from figures [61]. The accuracy of our method was tested by plotting a subset of data from Well *et al.* [51], re-extracting it, and then comparing it to the original values. The mean (min/max) difference (‰) was 0.06 (0.00/0.13) for $\delta^{15}N$ and 0.02 (0.00/0.07) for $\delta^{18}O$. This represents a worst-case accuracy of our ability to extract data from figures because the test data had an unusually wide range (−80 to +120‰ for $\delta^{15}N$, and 0 to +120‰ for $\delta^{18}O$; n = 53) and all other published graphs had much smaller scales. Values of $\delta^{18}O$-N_2O reported vs. atmospheric O_2 were converted to $\delta^{18}O$-N_2O vs. Vienna Standard Mean Ocean Water (VSMOW) according to Kim and Craig [19].

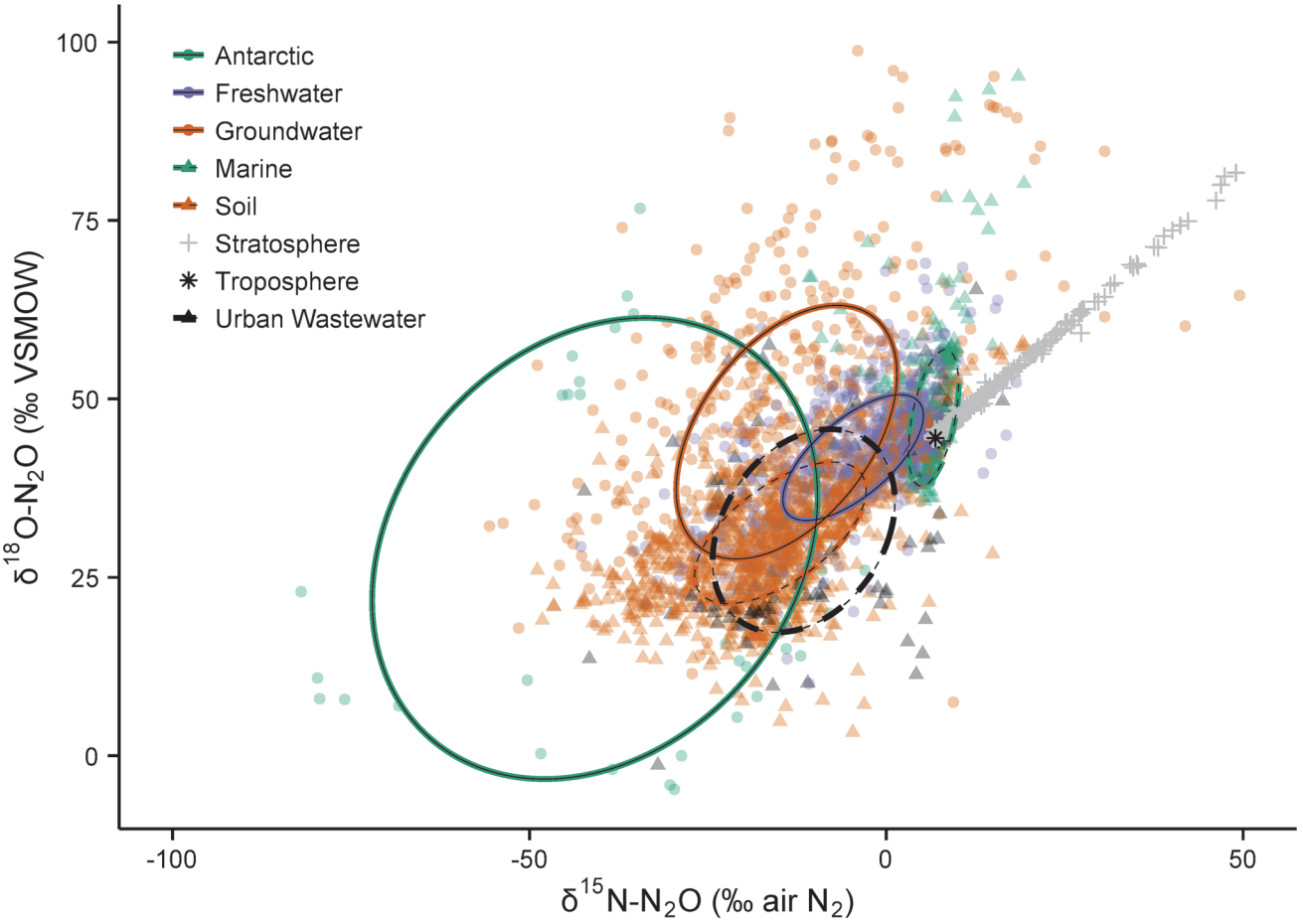

Fig 1. Global N_2O isotope measurements from atmospheric, marine, and terrestrial samples. All the data compiled in this study that fit within the axis ranges shown are plotted here. Each point represents one measurement, or in a few cases a reported average value, and is two-thirds transparent to allow the density of data to be displayed. Standard ellipses encompass ~40% of the data (Fig. 2) and are shown for the six non-atmospheric categories. Most data fall to the left of the current tropospheric value. Stratospheric data falls along a line ($\delta^{18}O = 0.89 \times \delta^{15}N + 38.4$) ($R^2 = 0.999$) that originates from the tropospheric value, and is caused by isotopic fractionation during N_2O destruction [13].

doi:10.1371/journal.pone.0118954.g001

Twenty-seven studies also measured the intramolecular distribution of ^{15}N in the linear NNO molecule (780 data points) and these data are provided in the supplementary datasets (S1 Dataset and S2 Dataset). This difference between the central ($\delta^{15}N^{\alpha}$) and terminal ($\delta^{15}N^{\beta}$) ^{15}N enrichment is often expressed as the site preference (SP). This parameter is thought to be a unique indicator of the microbial pathway that produces N_2O and not to be affected by variations in the isotopic ratios of substrates. Recently, this idea has been called into question by Yang *et al.* [62], who showed that SP can vary depending on the growth conditions of microbial cultures. Regardless, if the SP of different global sources is unique it can be used in conjunction with traditional measures of $\delta^{15}N\text{-}N_2O$ and $\delta^{18}O\text{-}N_2O$ values to separate sources in three-dimensional isotope space.

To this compendium of published data we added 1367 new *in situ* $\delta^{15}N\text{-}N_2O$ and $\delta^{18}O\text{-}N_2O$ data from 16 sites across Ontario and New Brunswick, Canada (S1 Dataset). Soil pore gas and static flux chambers were sampled at four Ontario sites. Urban wastewater treatment plants, streams, rivers, and agricultural drainage tile outlets were sampled across four watersheds in Ontario and New Brunswick. Groundwaters were sampled from numerous domestic

Table 1. Summary statistics of global $\delta^{15}N$-N_2O and $\delta^{18}O$-N_2O values as standard ellipses*.

Category	*n*	Sample-size-corrected ellipse area (‰ air N_2 × ‰ VSMOW)	Mean $\delta^{15}N$ ± 1σ (‰)	Mean $\delta^{18}O$ ± 1σ (‰)	Correlation (*r*)	Semi-major axis	Semi-minor axis	Slope of ellipse	Theta (θ, rads)
Stratosphere	288	44	20.31 ± 20.79	56.39 ± 18.44	0.9994	27.8	0.5	0.89	0.73
Troposphere	225	0.47	6.55 ± 0.47	44.40 ±0.34	0.3758	0.5	0.3	0.46	0.43
Soil	884	296	–14.85 ± 12.01	31.23 ± 9.89	0.6083	14.0	6.7	0.73	0.63
Freshwater	738	203	–4.65 ± 9.84	41.77 ± 8.79	0.6656	12.1	5.4	0.85	0.70
Marine	495	92	6.63 ± 3.50	47.35 ± 9.54	0.4866	9.7	3.0	5.05	1.38
Groundwater	530	768	–13.97 ± 15.46	45.34 ± 17.74	0.4552	20.2	12.1	1.35	0.93
Antarctic	35	3086	–40.84 ± 30.75	29.03 ± 31.82	0.2256	34.7	27.9	1.16	0.86
Urban Wastewater	92	545	–11.56 ± 12.70	31.51 ± 14.14	0.2922	15.4	11.2	1.43	0.96

*A visual description of the standard ellipse is found in Fig. 2.

doi:10.1371/journal.pone.0118954.t001

and monitoring wells (some multi-level) distributed across nine research sites in Ontario and New Brunswick.

Liquid samples were stripped of N_2O using an off-line purge-and-trap system described in Baulch *et al.* [35]. With the exception of samples from one location (ERS) that were analyzed at UC Davis-SIF, all analyses occurred at the University of Waterloo on an IsoPrime isotope ratio mass spectrometer (IRMS) with a TraceGas pre-concentrator with an analytical precision of 0.2‰ ($\delta^{15}N$-N_2O) and 0.4‰ ($\delta^{18}O$-N_2O). All samples were analyzed alongside an internal N_2O isotope standard that was previously calibrated at the University of Waterloo against local tropospheric air (assumed to be equal to 6.72‰ for $\delta^{15}N$ and 44.62‰ for $\delta^{18}O$ [17]). This internal standard gas was also submitted to UC Davis-SIF for isotopic analysis, and the standard deviation of 8 replicates (at varying concentrations including ambient) was 0.34‰ (for $\delta^{15}N$) and 0.77‰ (for $\delta^{18}O$). The absolute difference in the assigned value of this internal standard gas (blind inter-lab comparison) was 0.29‰ (for $\delta^{15}N$) and 0.81‰ (for $\delta^{18}O$). Given there are no internationally-recognized standardization methods or materials for N_2O isotope analysis, these inter-laboratory results are in good agreement with one another. All values are reported here in units of per mill (‰) relative to air-N_2 and VSMOW for $\delta^{15}N$ and $\delta^{18}O$, respectively.

All data were categorized as either Antarctic, freshwater, groundwater, marine, soil, stratosphere, troposphere, or urban wastewater, and a bivariate ellipse-based metric [63] was used to analyze and describe individual N_2O reservoirs (Table 1). This circular statistical analysis is an improvement over other techniques that qualitatively summarize isotope data with a polygon or a freeform shape e.g., [6,15,46,47]. There is often a high degree of covariance between $\delta^{15}N$-N_2O and $\delta^{18}O$-N_2O and this statistical technique provides an accurate description of the central tendency of the data. By definition, the standard ellipse contains ~40% of the data, is centered on the mean and has standard deviations of the bivariate data as semi-axes (Fig. 2) [63,64]. The data and an R file that contains the code to perform the statistical analyses and create the figures shown here are found at *https://github.com/jjvenky/Global-N2O-Ellipses*.

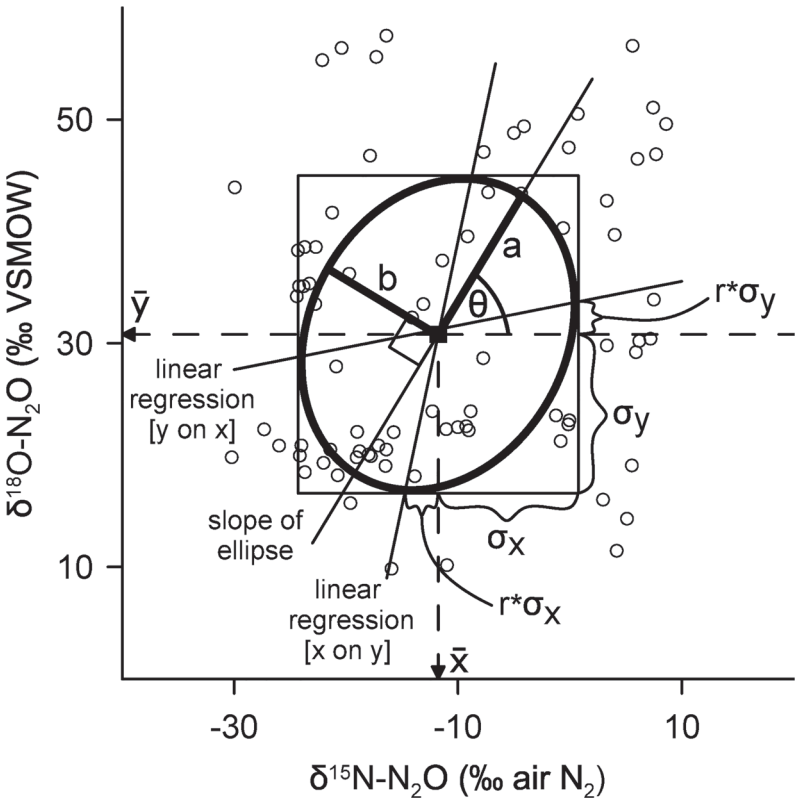

Fig 2. The standard ellipse of a bivariate sample. The urban wastewater N_2O isotope data from Townsend-Small *et al*. [41], Toyoda *et al*. [65], and this study ($n = 83$) are summarized here with a standard ellipse. The centre of the ellipse is located at the sample mean ($\bar{x}$, $\bar{y}$), where the semi-major (*a*) and semi-minor (*b*) axes intersect. The major axis is inclined versus the positive *x* axis by the angle θ. The tangent lines parallel to the *x* and *y* axes are related to the standard deviations (σ_x, σ_y) and the correlation coefficient (*r*). The two regression lines shown intersect the ellipse at the points of tangency [64].

doi:10.1371/journal.pone.0118954.g002

Results and Discussion

The data are highly non-uniform within and between categories (Figs. 1 and 3), and even within individual field sites (S1 Dataset). Historically, this has made it challenging to define an 'isotopic signature' for a given environment. Multiple factors cause this variability: (1) N_2O is produced by nitrification and denitrification, and the isotopic composition of N and oxygen (O) endmembers can vary widely [26,31,32,54]; (2) the apparent fractionation of $^{15}N/^{14}N$ and $^{18}O/^{16}O$ during N transformations is not constant, nor is it easily predicted; and (3) oxygen exchange between N_2O precursors and water imparts a large control on $\delta^{18}O\text{-}N_2O$ values during N_2O formation. While the exact mechanisms are not fully understood, it appears that greater amounts of exchange occur in unsaturated environments than in saturated ones [66–68]. Additionally, the reduction of N_2O to N_2 in anaerobic environments causes enrichment of ^{15}N and ^{18}O isotopes in the remaining N_2O pool, which displaces $\delta^{15}N\text{-}N_2O$ and $\delta^{18}O\text{-}N_2O$ values away from their original source values [26,51]. An initial analysis of all the data compiled in this study shows there is no clear separation of sources because each is described by an ellipse that overlaps at least one other source category (Figs. 1 and 3).

A similar comparison of all the published SP data (excluding Antarctic and groundwater categories) shows poor isotopic separation of sources (Fig. 4). It is difficult to determine how much of this variability is real, and how much is due to standardization issues and differences

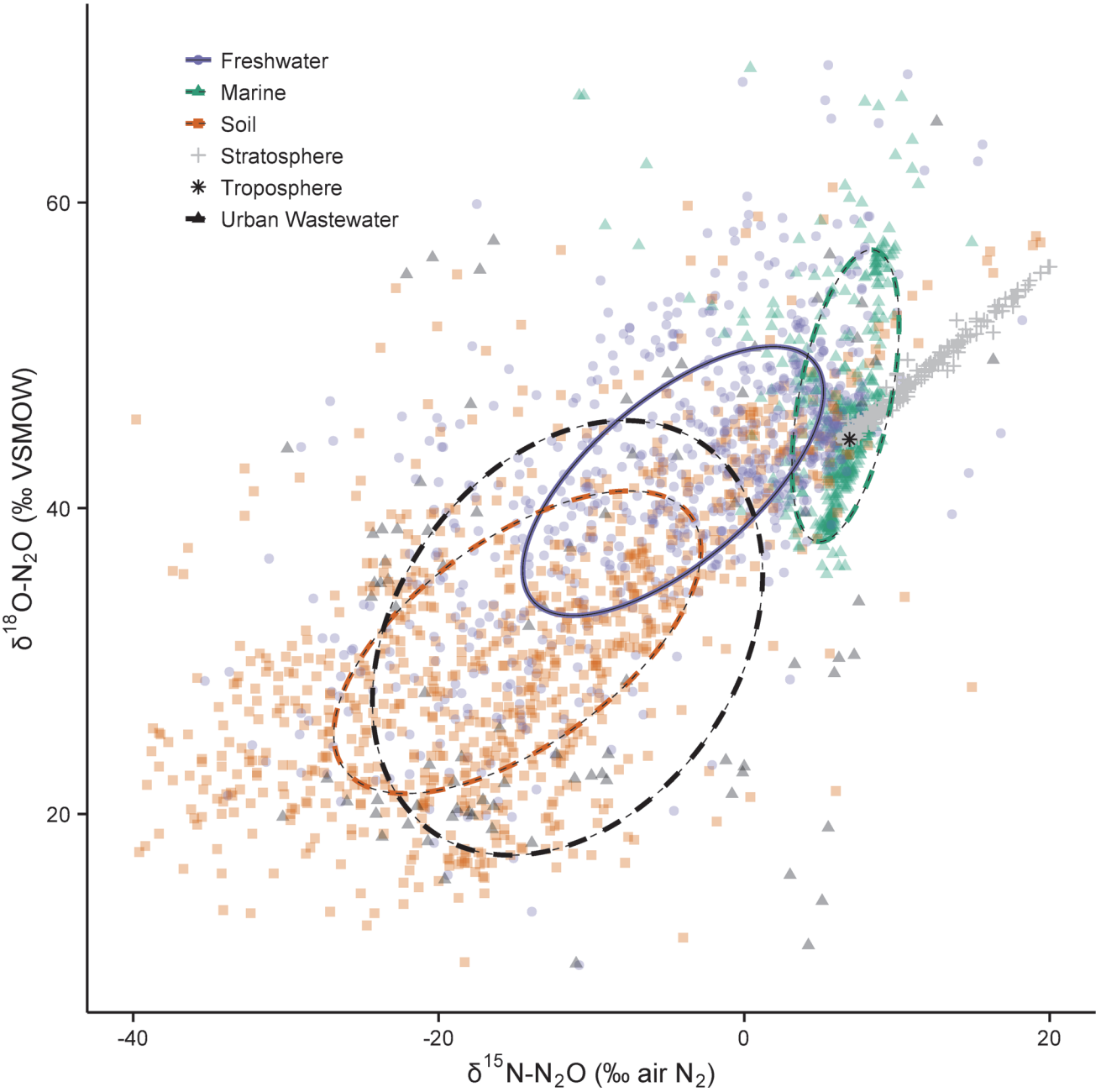

Fig 3. Global N_2O isotope measurements from atmospheric samples and key environmental sources: freshwater, marine and soil (n = 2117). Data from municipal wastewater treatment plants is also included (n = 92). Each point represents one measurement, or in a few cases a reported average value. The colour of each point is two-thirds transparent to allow the density of data to be displayed. Although the ellipses are the same as in Fig. 1, the scales of the axes are narrowed to better show the data relative to current atmospheric values.

doi:10.1371/journal.pone.0118954.g003

in measurement techniques. A recent inter-laboratory assessment of the methods used to determine nitrogen isotopomers revealed poor SP reproducibility [69]. Eleven laboratories employing either IRMS or laser spectroscopy techniques analyzed a single N_2O target gas and the resulting standard deviation for SP was 4.24‰. Further, the inter-lab variation in the mean SP value was high, spanning a range of 11.62‰ [69]. This may help explain why there are two distinct groupings of SP data in each of the troposphere [2,17] and the stratosphere [29,45,58]

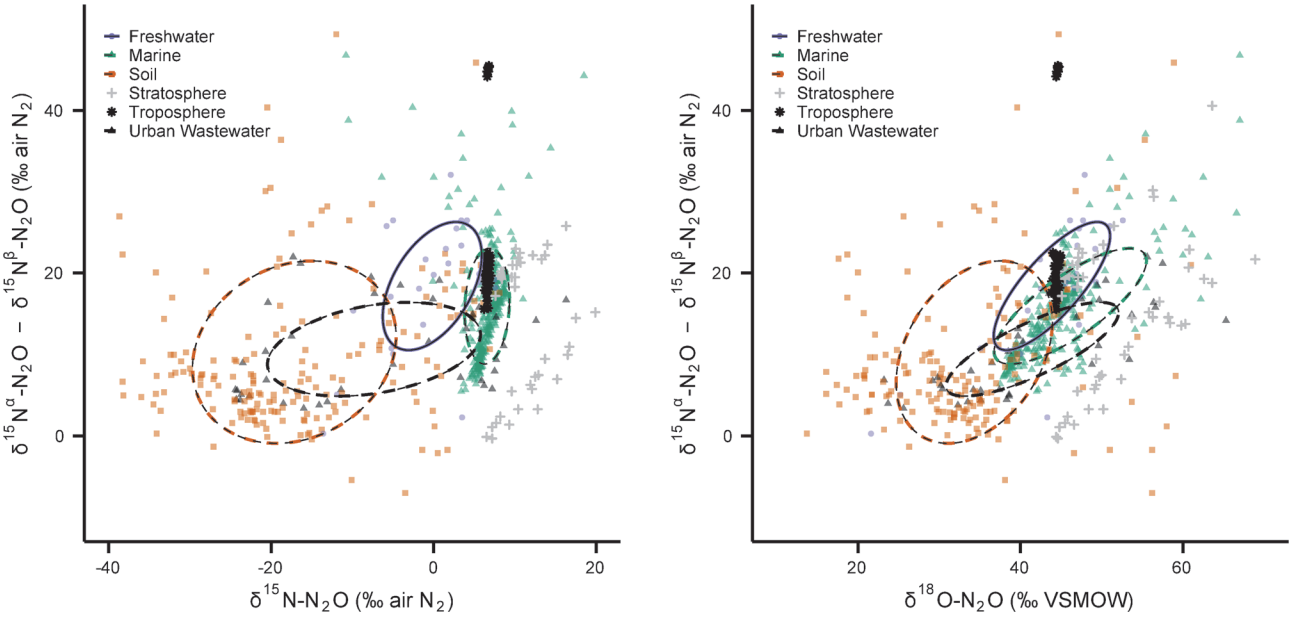

Fig 4. A comparison of ^{15}N site preference values (*y*-axes) and (a) $\delta^{15}N\text{-}N_2O$ (left panel) and (b) $\delta^{18}O\text{-}N_2O$ (right panel) measurements from freshwaters, oceans, soils, atmosphere, and urban wastewater (*n* = 651). Measurements of ^{15}N site preference from the Antarctic (*n* = 18) and groundwaters (*n* = 111) are not shown here, but are tabulated in S1 Dataset.

doi:10.1371/journal.pone.0118954.g004

(Fig. 4). Reaching an international consensus on standardization methods for the measurement and reporting of nitrogen isotopomers should vastly improve the utility of this data in source-apportionment studies at all scales. Finally, we note the reproducibility of $\delta^{15}N\text{-}N_2O$ and $\delta^{18}O\text{-}N_2O$ measurements in this recent round-robin test was much better than for SP, which gives us confidence in our ability to use these data here to make useful comparisons. The standard deviation (and range) of the N_2O target gas in the inter-lab comparison was 1.37‰ (1.89‰) for $\delta^{15}N\text{-}N_2O$ and 1.00‰ (3.47‰) for $\delta^{18}O\text{-}N_2O$ [69].

Much of the low concentration data from soils and surface waters are highly influenced by mixing with tropospheric N_2O. This is evident by the high density of soil, freshwater and marine data that lies near the tropospheric N_2O value (Fig. 3). In contrast, groundwater N_2O, which does not mix with the atmosphere following recharge, is unaffected by this mixing process. Other processes such as substrate enrichment and N_2O consumption control the isotopic composition of groundwater N_2O, which displays extreme variability even within the same location (Fig. 1) [50,51]. Only 15 studies reported flux-weighted average $\delta^{15}N\text{-}N_2O$, SP, and/or $\delta^{18}O\text{-}N_2O$ values, or provided enough information for us to calculate these values (2 freshwater studies, 2 marine studies, 10 soil studies, and 1 urban wastewater study; Fig. 5; S2 Dataset). The available flux-weighted data from soil and freshwater environments shows much overlap among this combined continental source, but the flux-weighted marine source appears to be unique. Importantly, there are very few flux-weighted data from all sources so robust conclusions cannot be made at this time. Additionally, these data were not weighted equally across studies so conclusions drawn from this analysis can be misleading. Only some of the values are time-weighted, and the sample size used to calculate the flux-weighted average varies from 3 to ~50 (S2 Dataset). Emissions of N_2O from soils (and potentially freshwaters and oceans) are inherently episodic, so future estimates of the flux-weighted average should attempt to include multiple measurements made over long timescales (months to years and encompassing seasonal differences) whenever possible.

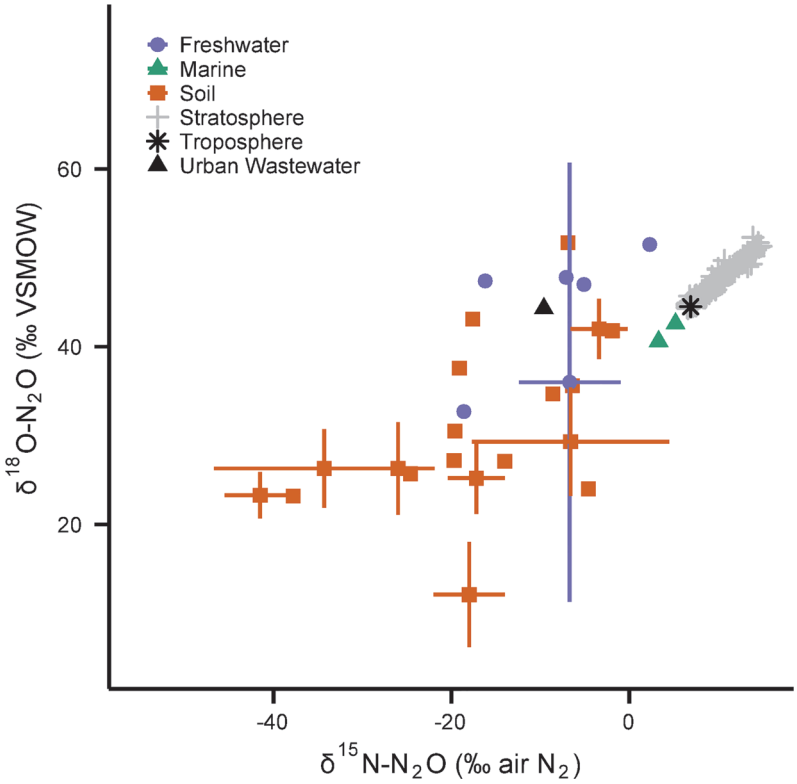

Fig 5. Emission-weighted average δ^{15}N-N_2O and δ^{18}O-N_2O from continental and marine environments. A small number of studies reported flux-weighted or flux and time-weighted average values. A few other studies provided information that allowed us to calculate these values. Equal weighting criteria were not applied in each case because not all values are time-weighted. Additional factors such as the sample size (*n*), antecedent conditions of N_2O substrate(s), and time of year also different among studies (see S2 Dataset).

doi:10.1371/journal.pone.0118954.g005

The results of our analyses shown in Figs. 1 and 3 are not flux-weighted, nor are all the categories important atmospheric sources. For example, the most recent IPCC assessment reports that human excreta (all forms of treated/untreated sewage) contributes between 0.1–0.3 Tg N yr^{-1} as N_2O, or only ~1.1% of all natural and anthropogenic sources [5]. Of this, N_2O emissions from urban wastewater treatment plants constitutes a very small fraction. To address this, we analyzed subsets of the data from important atmospheric sources (freshwaters, oceans, and soils) that were not strongly influenced by mixing with tropospheric N_2O, and thereby make an important contribution to the flux-weighted average source value (Table 2; Fig. 6). To do this we filtered the data to include: (i) all reports of emitted N_2O, regardless of the strength of the flux (two freshwater studies [13,46], two marine studies [16,43] and several soil studies) (see S2 Dataset); (ii) isotope data in the soil profile that had concentrations of N_2O >650 ppb v/v (or 200% ambient); and (iii) isotope data in freshwater and near-surface marine environments (depths >100 m) with dissolved N_2O concentrations >200% saturation with respect to atmospheric N_2O [70].

Most of the freshwater and soil data were retained (71% and 90%, respectively), and the ellipses of these data subsets are similar to the ellipses for all data in these categories (Table 1). Although the median δ^{15}N and δ^{18}O values of freshwater and soil N_2O are significantly different ($p < 0.001$, Mann-Whitney test), their ellipses intersect one another at the 1σ level (Fig. 6–top panel), and we conclude that these sources are not isotopically distinct at the global scale.

Table 2. Summary statistics of filtered $\delta^{15}N$-N_2O and $\delta^{18}O$-N_2O data. These values show a subset of data that were not strongly influenced by mixing with tropospheric N_2O, and thereby make an important contribution to the flux-weighted average source value (see Fig. 6).

Category	*n*	Sample-size-corrected ellipse area (‰ air N_2 × ‰ VSMOW)	Mean $\delta^{15}N$ ± 1σ (‰)	Mean $\delta^{18}O$ ± 1σ (‰)	Correlation (*r*)	Semi-major axis	Semi-minor axis	Slope of ellipse	Theta (θ, rads)
Soil	794	288	−16.66 ± 11.24	30.05 ± 9.63	0.5341	13.0	7.0	0.75	0.64
Freshwater	527	215	−7.78 ± 9.72	40.75 ± 9.63	0.6821	12.5	5.5	0.99	0.78
Marine	62	22	5.14 ± 1.93	44.76 ± 3.62	0.0435	3.6	1.9	30.87	1.54
Continental*	1321	299	−13.11 ± 11.51	34.32 ± 10.96	0.6577	14.5	6.6	0.93	0.75

*The continental source, operationally defined here as Soil + Freshwater, is used along with the Marine source in our box-model calculations.

doi:10.1371/journal.pone.0118954.t002

In order to further delineate freshwater and soil N_2O more stable isotope measurements from freshwaters are needed; especially from non-temperate environments because the current data coverage from these systems is lacking. Measurements of SP may prove to be a useful means of separating these sources because the ellipses that describe SP vs. $\delta^{15}N_{bulk}$ for freshwater and soils do not overlap (Fig. 6–middle panel).

Of the 495 published marine values compiled here, only 62 originated from the top 100 m of the ocean and were >200% saturation. Relative to continental N_2O sources, the $\delta^{15}N$ and $\delta^{18}O$ values of near-surface oceanic N_2O sources are poorly constrained. We found no reports of N_2O isotope values from estuaries, which could represent an important fraction of the marine source but should be similar to marine or freshwater values. Tropical systems including reservoirs are also poorly studied. Future campaigns to more fully characterize $\delta^{15}N$ and $\delta^{18}O$ values of N_2O emissions from aquatic environments, especially those impacted by anthropogenic N sources, are needed.

Although N_2O generated from fossil fuel and biomass combustion may contribute ~8% of the total source (or ~20% of the anthropogenic source [5]), its isotopic composition is largely unknown. A lab-scale investigation of coal combustion revealed $\delta^{15}N$-N_2O and $\delta^{18}O$-N_2O values that were both enriched (unstaged combustion) and slightly depleted (air-staged combustion) relative to tropospheric N_2O [71], indicating coal-derived N_2O isotope values might be similar to marine sources but are dependent upon combustion conditions. A controlled study of gasoline-powered automobile exhaust concluded the average $\delta^{15}N$-N_2O and $\delta^{18}O$-N_2O values are similar to freshwater sources (−4.9 ±8.2‰ and +43.5 ± 13.9‰, respectively) [72]. Finally, N_2O derived from biomass burning appears to closely resemble the $\delta^{15}N$ and $\delta^{18}O$ values of its endmembers; biomass-N and atmospheric O_2, respectively [73]. We recognize the need to further investigate these potentially important sources and evaluate how they might affect the global N_2O isotope budget.

After analyzing the filtered $\delta^{15}N$-N_2O and $\delta^{18}O$-N_2O data, the 'bottom-up' global N_2O sources defined here were compared to estimates derived from 'top-down' atmospheric models (Fig. 7). Modelled estimates of the average anthropogenic and natural source fall within (or very close to) the soil ellipse *and* along a mixing line between soil and tropospheric N_2O. All but two of the modelled estimates fall outside the freshwater ellipse, indicating the bulk of the combined anthropogenic and natural sources are not from freshwaters. If freshwaters were a major source of atmospheric N_2O, a mixing line between freshwater and tropospheric N_2O would be much closer to the anthropogenic and natural source values. It is not, and therefore

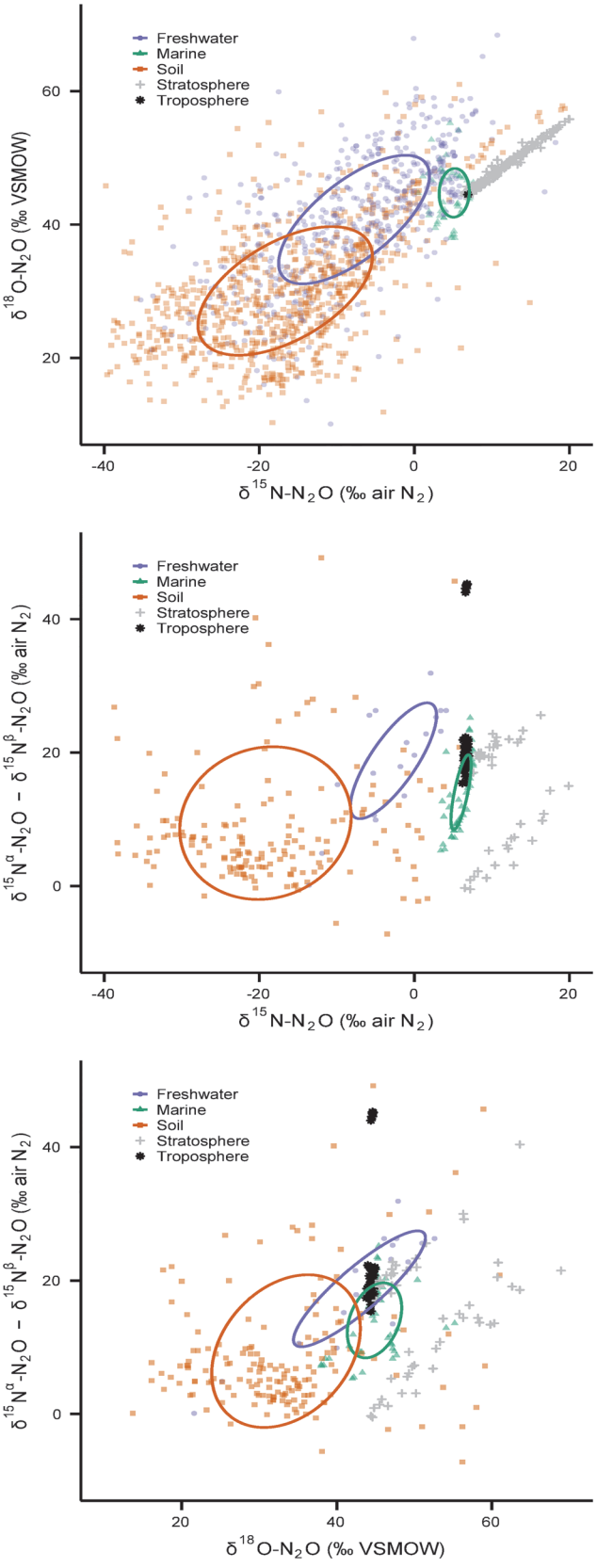
Freshwater
Marine
Soil
Stratosphere
Troposphere
δ18O-N2O (‰ VSMOW)
δ15N-N2O (‰ air N2)
δ15Nα-N2O − δ15Nβ-N2O (‰ air N2)

Fig 6. Nitrous oxide isotope measurements of key sources in the global isotope budget. Soil, freshwater and marine data were filtered to exclude samples that were highly influenced by mixing with tropospheric N_2O: (a) $\delta^{15}N\text{-}N_2O$ vs. $\delta^{18}O\text{-}N_2O$ (top panel, $n = 1383$); (b) SP vs. $\delta^{15}N\text{-}N_2O$ (middle panel; $n = 235$); and (c) SP vs. $\delta^{18}O\text{-}N_2O$ (bottom panel; $n = 235$). The filtering criteria are described in the text.

doi:10.1371/journal.pone.0118954.g006

we confirm what 'top-down' approaches have previously inferred: soil is the main source of N_2O to the atmosphere.

We used the newly constrained $\delta^{15}N\text{-}N_2O$ and $\delta^{18}O\text{-}N_2O$ values for freshwater and soil (the combined continental source) and the ocean source to model their relative contributions to the total annual flux of N_2O. We began with a box-model approach similar to that presented in [8,9,11,29]. We adapted the following isotope mass-balance equation for atmospheric N_2O from Park *et al.* [29]:

$$Burden \times \frac{\partial \delta_{Trop}}{\partial t} = \sum Sources(\delta_{Sources} - \delta_{Trop}) - (\varepsilon \times L) \quad (1)$$

where,*Burden* = Present-day burden of N_2O in the troposphere [1553 (± 21.742) Tg N] as reported by Stocker *et al.* [5]. This estimate is for year 2011, and is updated from data provided in Prather *et al.* [74], who report an uncertainty of 1.4% for year 2010.

$\frac{\partial \delta_{Trop}}{\partial t}$ = Deseasonalized, linear trend in archived samples of tropospheric N_2O measured by Park *et al.* [2]. The linear trends for $\delta^{15}N\text{-}N_2O$ and $\delta^{18}O\text{-}N_2O$ are −0.035‰ yr^{-1} (± 0.002) and −0.022‰ yr^{-1} (± 0.004), respectively.

$\sum$ *Source* = Annual N_2O emissions from all sources (17.9 Tg N yr^{-1}) [5]. For our calculations we applied an uncertainty of 25% to this parameter.

$\delta_{Sources}$ = Flux-weighted $\delta^{15}N\text{-}N_2O$ or $\delta^{18}O\text{-}N_2O$ value (‰) of the average modern source (all natural and anthropogenic sources).

δ_{Trop} = $\delta^{15}N\text{-}N_2O$ or $\delta^{18}O\text{-}N_2O$ value (‰) of the modern troposphere (provided in Table 1).

ε = Apparent enrichment factor (‰) for N_2O destruction processes in the stratosphere. These values are taken from Table 3 in Park *et al.* [29], and are −14.9‰ (± 0.5) for ^{15}N and −13.5‰ (± 0.5) for ^{18}O. Note, the ratio of enrichment factors provided by Park *et al.* [29] (^{18}O: $^{15}N = 0.906$) is very close to the slope of the regression line of the stratospheric N_2O data shown in Fig. 1 ($\delta^{18}O\text{-}N_2O$:$\delta^{15}N\text{-}N_2O = 0.886$).

L = Photochemical loss rate of N_2O in the stratosphere (14.3 Tg N yr^{-1}) [5]. Following [29], we applied an uncertainty of 25% in our calculations.

The term $(-\varepsilon \times L)$ is a very close approximation of the 'Net Isotope Flux' (‰ Tg N yr^{-1}) as defined in [29], and is the net annual flux of N_2O isotopologues from the stratosphere to the troposphere.

Equation 1 can be rearranged to solve for $\delta_{Sources}$ (Eq. 2), and all the known quantities provided above can be substituted into Eq. 2 to derive a flux-weighted, average modern source value ($\delta_{Sources}$) for $\delta^{15}N\text{-}N_2O$ and $\delta^{18}O\text{-}N_2O$ (‰).

$$\delta_{Sources} = \frac{\left(Burden \times \frac{\partial \delta_{Trop}}{\partial t}\right) + (\varepsilon \times L) + (\sum Sources \times \delta_{Trop})}{\sum Sources} \quad (2)$$

Accordingly, we derive an average modern source value (± propagated standard deviation) for $\delta^{15}N\text{-}N_2O$ and $\delta^{18}O\text{-}N_2O$ of −8.4‰ (± 4.0) and +31.7‰ (± 13.9), respectively.

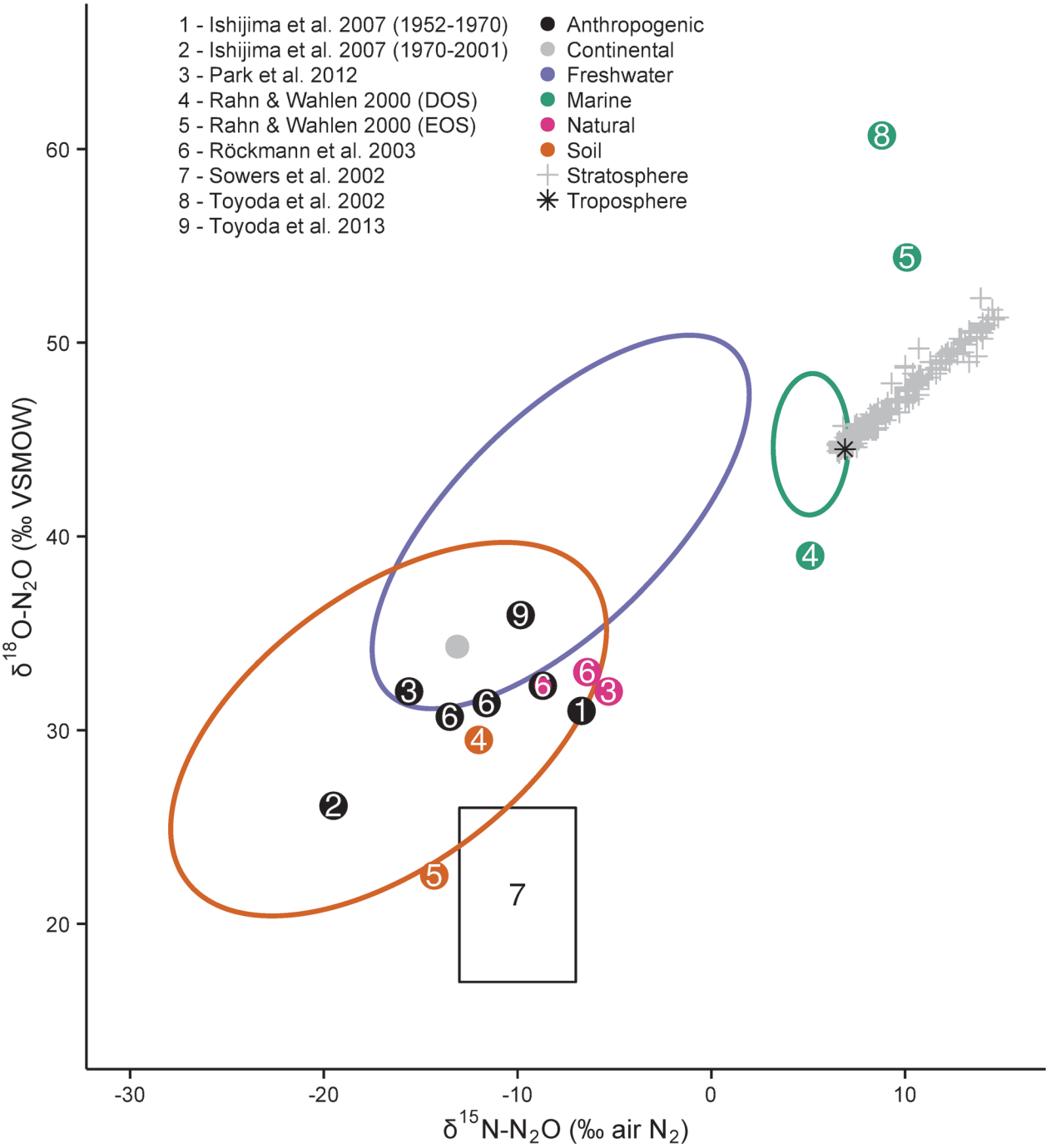

Fig 7. A comparison of bottom-up measurements to top-down estimates of N_2O sources. Previous top-down studies have used a variety of modelling approaches to apportion the global N_2O budget into different sources, identified here by colour. Ishijima *et al*. [10] measured N_2O in firn air and calculated the isotopic composition of the anthropogenic source for two time periods: 1952 1970 and 1970 2001 that differed markedly in $\delta^{15}N$. Park et al. [2] constrained the pre-industrial, natural N_2O source from $\delta^{15}N$-N_2O and $\delta^{18}O$-N_2O measurements in firn air and then calculated the current anthropogenic N_2O source using recent archived air samples. Rahn and Wahlen [6] evaluated a depleted ocean scenario [DOS, originally proposed by Kim and Craig [20]], and an enriched ocean scenario [EOS, originally proposed by Kim and Craig [19]] to calculate corresponding terrestrial N_2O sources. Röckmann *et al*. [9] measured N_2O in firn air and modelled the pre-industrial (natural) source, the modern global average source (pink circle with black outline), and the anthropogenic source under the IPCC3 (higher value) and IPCC2 (lower value) scenarios. Sowers *et al*. [11] measured firn air and gas trapped in an ice core to calculate a range of values for the isotopic composition of the average anthropogenic N_2O source. Toyoda *et al*. [7] estimated the $\delta^{15}N$ and $\delta^{18}O$ value of the oceanic N_2O source using 'Keeling Plots' of detailed water column data. Toyoda *et al*. [8] monitored the isotopic ratio of tropospheric N_2O in the northern hemisphere on a monthly basis from 2000–2011, and then used a box-model to estimate the current anthropogenic source. For reference, we show the Continental N_2O source, which is used along with the Marine source in our box-model calculations, and is operationally defined as Soil + Freshwater.

doi:10.1371/journal.pone.0118954.g007

Table 3. MixSIAR model output summary.

	Category	Mean Contribution	Standard Deviation (σ)	Confidence Interval						
				2.5%	5%	25%	50%	75%	95%	97.5%
2-isotope ($\delta^{15}N_{bulk}$, $\delta^{18}O$) mixing model	Soil	0.34	0.23	0.02	0.03	0.15	0.31	0.51	0.77	0.83
	Freshwater	0.24	0.16	0.01	0.02	0.11	0.22	0.35	0.51	0.57
	Marine	0.42	0.21	0.03	0.07	0.26	0.43	0.58	0.77	0.83
3-isotope ($\delta^{15}N_{bulk}$, $\delta^{18}O$, SP) mixing model	Soil	0.33	0.22	0.02	0.03	0.15	0.31	0.49	0.72	0.78
	Freshwater	0.24	0.16	0.01	0.02	0.11	0.21	0.35	0.53	0.59
	Marine	0.43	0.19	0.07	0.13	0.30	0.42	0.55	0.75	0.82

doi:10.1371/journal.pone.0118954.t003

If we were to assume that all N_2O fluxes *(F)* originate only from marine and continental sources, then:

$$\sum Sources \approx F_{Ocean} + F_{Cont} \approx 17.9 \text{ Tg N yr}^{-1} \quad (3)$$

and the flux-weighted modern source value is approximated by:

$$\delta_{Sources} \approx \frac{(\delta_{Cont} \times F_{Cont}) + (\delta_{Ocean} \times F_{Ocean})}{\sum Sources} \quad (4)$$

where the δ value of the continental and ocean sources are given in Table 2.

Combining Eq. 2 with Eq. 4 yields:

$$(\delta_{Cont} \times F_{Cont}) + (\delta_{Ocean} \times F_{Ocean}) \approx \left(Burden \times \frac{\partial \delta_{Trop}}{\partial t}\right) + (\varepsilon \times L) + \left(\sum Sources \times \delta_{Trop}\right) \quad (5)$$

Given the assumption that $F_{Cont} \approx \sum Sources - F_{Ocean}$ (Eq. 3), we can approximate F_{ocean} by:

$$F_{Ocean} \approx \frac{\left(Burden \times \frac{\partial \delta_{Trop}}{\partial t}\right) + (\varepsilon \times L) + \sum Sources(\delta_{Trop} - \delta_{Cont})}{\delta_{Ocean} - \delta_{Cont}} \quad (6)$$

Accordingly, using N isotope ratios we derive a value for F_{ocean} of ∼4.6 (± 12.6) Tg N yr^{-1}, which is ∼26% of all sources (17.9 Tg N yr^{-1}) [5]. The F_{Cont} is found by difference, and is approximately equal to 13.3 (± 13.4) Tg N yr^{-1}, or 74% of all natural and anthropogenic N_2O sources. The largest source of uncertainty in the N isotope mass-balance lies in the $\delta^{15}N$ value of the continental source (1σ = 11.5‰), followed by ∑ *Sources* and *L*, which have a relative uncertainty of 25% in our model.

The most recent N_2O budget estimates the combined soil, freshwater, and ocean flux to be ∼15.7 Tg N yr^{-1}, or 87.7% of the total source [5]. Our approach assumes the ∑ *Sources* = 17.9 Tg N yr^{-1} (as reported in IPCC-AR5) because other terms in the mass-balance (e.g., N_2O burden and loss rate) are based on a budget that includes all known sources. As such, we ignore the contributions from smaller sources such as human sewage, fossil fuels, industry, biomass combustion, and chemical production processes in the atmosphere, which have a combined annual flux of ∼2.2 Tg N yr^{-1} [5]. Despite this, our result for F_{ocean} is similar to the estimate provided in IPCC-AR5, which shows oceans contribute 21% of the annual N_2O budget [5].

The O isotope mass-balance fails to derive a positive ocean flux (F_{ocean} = −4.5 ± 19.9 Tg N yr^{-1}). This is because the $\delta^{18}O$ separation between the troposphere and the continental source is smaller than it is for $\delta^{15}N$, and the term ∑ *Sources* ($\delta_{Trop} - \delta_{Cont}$) is too small to make the numerator in Eq. 6 a net positive number. However, decreasing the loss rate (*L*) by 4 Tg N

yr^{-1} and increasing Σ *Sources* by the same amount yields a positive ocean flux = 4.6 Tg N yr^{-1}. Therefore, if the uncertainty of these parameters is reduced in the future we may find that the O isotope budget balances.

Finally, we used a stable isotope Bayesian mixing model (MixSIAR) [75] to determine the proportions of soil, freshwater, and marine N_2O that best predicted the average modern source (anthropogenic plus natural) (Eq. 7).

$$\delta_{Sources} = (\delta_{Soil} \times F_{Soil}) + (\delta_{Freshwater} \times F_{Freshwater}) + (\delta_{Ocean} \times F_{Ocean}) \quad (7)$$

where, $F_{Soil} + F_{Freshwater} + F_{Ocean} = 1$.

MixSIAR, which is a front-end interface of the model SIAR (Stable Isotope Analysis in R) [76], is an ecological mixing model traditionally used to describe food web and predator-prey relationships. Values of $\delta^{15}N_{bulk}$-N_2O, $\delta^{15}N^{\alpha}$-N_2O, $\delta^{15}N^{\beta}$-N_2O, and $\delta^{18}O$-N_2O for the average modern source (the mixture) were taken from Röckmann *et al.* [9]. These estimates are almost identical to the ones calculated in our 2-box-model (above), and Röckmann *et al.* [9] provided ^{15}N isotopomers, which allowed us to use 3 variables in our model runs ($\delta^{15}N_{bulk}$, $\delta^{18}O$, and SP). A series of Markov Chain Monte Carlo simulations, using values for soil, freshwater, and marine N_2O (filtered, raw data compiled in this study), were done to find mixing solutions that best fit the average modern source (Table 3). Gelman-Rubin and Geweke diagnostic tests indicated a chain length of 300,000, burn in of 200,000, thinning of 50 (2-isotope) or 100 (3-isotope), and 3 chains were appropriate.

Model runs using only the $\delta^{15}N$-N_2O and $\delta^{18}O$-N_2O data (2-isotope mixing model, n = 1383 data pairs) produced results very similar to the model runs that also included SP data (3-isotope mixing model, n = 235 data triads). Overall, this Bayesian modeling exercise predicted the soil, freshwater, and ocean contributions (± 1σ) to the average modern N_2O source were 0.43 (0.20), 0.34 (0.22), and 0.24 (0.16), respectively (Table 3). Unlike the box-model, this approach does not place *a priori* bounds on the data, and is not constrained by terms such as the stratospheric N_2O loss rate (L), which have large uncertainty. However, this method also ignores the contributions of several small sources, which have a combined contribution of ~12.3% to the total budget presented in IPCC-AR5 [5].

Both SIAR and the box-model predict the ocean flux to be 24% and 26% of the total, respectively, which closely confirms the scientific community's best estimate of the ocean flux as presented in IPCC-AR5 (21% of the total source). Further, the SIAR model output shows that freshwaters may contribute much more N_2O than previously thought. The current N_2O budget estimates the combined flux from rivers, estuaries, and coastal zones is 0.6 Tg N yr^{-1}, or just 3% of the total source. While we acknowledge that there is $\delta^{15}N$-$\delta^{18}O$ overlap in the soil and freshwater source (Fig. 6–top and bottom panels), these sources appear to be unique in $\delta^{15}N$-SP space (Fig. 6–middle panel). Therefore, we suggest there is a great need to quantify N_2O fluxes from freshwaters, estuaries, and coastal zones, which have received considerably less attention than soil and off-shore marine environments.

Supporting Information

S1 Dataset. A comma-delimited text file with all the data collected and analyzed in this study. In addition to $\delta^{15}N$-N_2O, SP and $\delta^{18}O$-N_2O values, we provide a reference citation, the category, a brief site description, and the criteria used to filter the data subsets (S1_Dataset.csv).
(CSV)

S2 Dataset. A comma-delimited text file with weighted average $\delta^{15}N$-N_2O, SP and $\delta^{18}O$-N_2O values from select freshwater, soil and urban wastewater studies (S2_Dataset.csv).
(CSV)

Acknowledgments

We thank the following people for their contributions in obtaining the new data presented in this study: R. Aravena, R. Elgood, J. Harbin, M. Levesque, W. Mark, M. Rempel, W. Robertson, M. Rosamond, A. Rossi, N. Senger, S. Thuss, A. Vandenhoff, and C. Wagner-Riddle. We are indebted to Hadley Wickham for the creation of ggplot2; an implementation of the Grammar of Graphics in R. We are especially grateful to all the anonymous reviewers who provided us with helpful suggestions as this manuscript evolved.

Author Contributions

Conceived and designed the experiments: DMS JJV SLS JS. Performed the experiments: DMS JJV. Analyzed the data: DMS JJV. Wrote the paper: DMS JJV SLS JS.

References

1. Fowler D, Coyle M, Skiba U, Sutton MA, Cape JN, Reis S, et al. The global nitrogen cycle in the twenty-first century. Philos Trans R Soc B Biol Sci. 2013; 368: 20130164–20130164. doi:10.1098/rstb.2013.0164 PMID: 23713126
2. Park S, Croteau P, Boering KA, Etheridge DM, Ferretti D, Fraser PJ, et al. Trends and seasonal cycles in the isotopic composition of nitrous oxide since 1940. Nat Geosci. 2012; 5: 261–265. doi:10.1038/ngeo1421
3. Ravishankara AR, Daniel JS, Portmann RW. Nitrous Oxide (N_2O): The dominant ozone-depleting substance emitted in the 21st century. Science. 2009; 326: 123–125. doi:10.1126/science.1176985 PMID: 19713491
4. Prinn RG, Weiss RF, Fraser PJ, Simmonds PG, Cunnold DM, Alyea FN, et al. A history of chemically and radiatively important gases in air deduced from ALE/GAGE/AGAGE. J Geophys Res Atmospheres. 2000; 105: 17751–17792. doi:10.1029/2000JD900141
5. Stocker TF, Qin D, Plattner G-K, Tignor M, Allen SK, Boschung J, et al., editors. Climate Change 2013: The Physical Science Basis. Contributions of Working Group I to the Fifth Assessment Report of the Intergovernmental Panel on Climate Change. Cambridge, United Kingdom and New York, NY, USA: Cambridge University Press; 2013. 1535 p.
6. Rahn T, Wahlen M. A reassessment of the global isotopic budget of atmospheric nitrous oxide. Glob Biogeochem Cycles. 2000; 14: 537–543. doi:10.1029/1999GB900070
7. Toyoda S, Yoshida N, Miwa T, Matsui Y, Yamagishi H, Tsunogai U. Production mechanism and global budget of N_2O inferred from its isotopomers in the western North Pacific. Geophys Res Lett. 2002; 29: 7-1–7-4. doi:10.1029/2001GL014311
8. Toyoda S, Kuroki N, Yoshida N, Ishijima K, Tohjima Y, Machida T. Decadal time series of tropospheric abundance of N_2O isotopomers and isotopologues in the Northern Hemisphere obtained by the long-term observation at Hateruma Island, Japan. J Geophys Res Atmospheres. 2013; 118: 3369–3381. doi:10.1002/jgrd.50221
9. Röckmann T, Kaiser J, Brenninkmeijer CAM. The isotopic fingerprint of the pre-industrial and the anthropogenic N_2O source. Atmospheric Chem Phys. 2003; 3: 315–323.
10. Ishijima K, Sugawara S, Kawamura K, Hashida G, Morimoto S, Murayama S, et al. Temporal variations of the atmospheric nitrous oxide concentration and its delta N-15 and delta O-18 for the latter half of the 20th century reconstructed from firn air analyses. J Geophys Res-Atmospheres. 2007; 112. doi:10.1029/2006JD007208
11. Sowers T, Rodebaugh A, Yoshida N, Toyoda S. Extending records of the isotopic composition of atmospheric N_2O back to 1800 A.D. from air trapped in snow at the South Pole and the Greenland Ice Sheet Project II ice core. Glob Biogeochem Cycles. 2002; 16: 76-1–76-10. doi:10.1029/2002GB001911
12. Boontanon N, Ueda S, Kanatharana P, Wada E. Intramolecular stable isotope ratios of N_2O in the tropical swamp forest in Thailand. Naturwissenschaften. 2000; 87: 188–192. doi:10.1007/s001140050701 PMID: 10840807

13. Rahn T, Wahlen M. Stable isotope enrichment in stratospheric nitrous oxide. Science. 1997; 278: 1776–1778. doi:10.1126/science.278.5344.1776 PMID: 9388175

14. Croteau P, Atlas EL, Schauffler SM, Blake DR, Diskin GS, Boering KA. Effect of local and regional sources on the isotopic composition of nitrous oxide in the tropical free troposphere and tropopause layer. J Geophys Res. 2010; 115. doi:10.1029/2009JD013117 PMID: 20463844

15. Dore JE, Popp BN, Karl DM, Sansone FJ. A large source of atmospheric nitrous oxide from subtropical North Pacific surface waters. Nature. 1998; 396: 63–66. doi:10.1038/23921

16. Frame CH, Deal E, Nevison CD, Casciotti KL. N_2O production in the eastern South Atlantic: Analysis of N_2O stable isotopic and concentration data. Glob Biogeochem Cycles. 2014; 28. doi:10.1002/2013GB004790

17. Kaiser J, Röckmann T, Brenninkmeijer CAM. Complete and accurate mass spectrometric isotope analysis of tropospheric nitrous oxide. J Geophys Res. 2003; 108. doi:10.1029/2003JD003613 PMID: 14686320

18. Kaiser J, Engel A, Borchers R, Röckmann T. Probing stratospheric transport and chemistry with new balloon and aircraft observations of the meridional and vertical N_2O isotope distribution. Atmospheric Chem Phys. 2006; 6: 3535–3556.

19. Kim K, Craig H. Two-isotope characterization of N_2O in the Pacific Ocean and constraints on its origin in deep water. Nature. 1990; 347: 58–61. doi:10.1038/347058a0

20. Kim K, Craig H. Nitrogen-15 and Oxygen-18 characteristics of nitrous oxide: a global perspective. Science. 1993; 262: 1855–1857. doi:10.1126/science.262.5141.1855 PMID: 17829632

21. Koba K, Osaka K, Tobari Y, Toyoda S, Ohte N, Katsuyama M, et al. Biogeochemistry of nitrous oxide in groundwater in a forested ecosystem elucidated by nitrous oxide isotopomer measurements. Geochim Cosmochim Acta. 2009; 73: 3115–3133. doi:10.1016/j.gca.2009.03.022

22. Koehler B, Corre MD, Steger K, Well R, Zehe E, Sueta JP, et al. An in-depth look into a tropical lowland forest soil: nitrogen-addition effects on the contents of N_2O, CO_2 and CH_4 and N_2O isotopic signatures down to 2-m depth. Biogeochemistry. 2012; 111: 695–713. doi:10.1007/s10533-012-9711-6

23. Li L, Spoelstra J, Robertson WD, Schiff SL, Elgood RJ. Nitrous oxide as an indicator of nitrogen transformation in a septic system plume. J Hydrol. 2014; 519: 1882–1894. doi:10.1016/j.jhydrol.2014.09.037

24. Maeda K, Toyoda S, Shimojima R, Osada T, Hanajima D, Morioka R, et al. Source of nitrous oxide emissions during the cow manure composting process as revealed by isotopomer analysis of and amoa abundance in betaproteobacterial ammonia-oxidizing bacteria. Appl Environ Microbiol. 2010; 76: 1555–1562. doi:10.1128/AEM.01394-09 PMID: 20048060

25. Mander Ü, Well R, Weymann D, Soosaar K, Maddison M, Kanal A, et al. Isotopologue ratios of N_2O and N_2 measurements underpin the importance of denitrification in differently N-loaded riparian alder forests. Environ Sci Technol. 2014; 48: 11910–11918. doi:10.1021/es501727h PMID: 25264900

26. Mandernack KW, Rahn T, Kinney C, Wahlen M. The biogeochemical controls of the $\delta^{15}N$ and $\delta^{18}O$ of N_2O produced in landfill cover soils. J Geophys Res-Atmospheres. 2000; 105: 17709–17720. doi:10.1029/2000JD900055

27. Naqvi SWA, Yoshinari T, Jayakumar DA, Altabet MA, Narvekar PV, Devol AH, et al. Budgetary and biogeochemical implications of N_2O isotope signatures in the Arabian Sea. Nature. 1998; 394: 462–464. doi:10.1038/28828

28. Ostrom NE, Sutka R, Ostrom PH, Grandy AS, Huizinga KM, Gandhi H, et al. Isotopologue data reveal bacterial denitrification as the primary source of N_2O during a high flux event following cultivation of a native temperate grassland. Soil Biol Biochem. 2010; 42: 499–506. doi:10.1016/j.soilbio.2009.12.003

29. Park S, Atlas EL, Boering KA. Measurements of N_2O isotopologues in the stratosphere: Influence of transport on the apparent enrichment factors and the isotopologue fluxes to the troposphere. J Geophys Res. 2004; 109. doi:10.1029/2003JD003731

30. Park S, Pérez T, Boering KA, Trumbore SE, Gil J, Marquina S, et al. Can N_2O stable isotopes and isotopomers be useful tools to characterize sources and microbial pathways of N_2O production and consumption in tropical soils? Glob Biogeochem Cycles. 2011; 25, GB1001. doi:10.1029/2009GB003615

31. Pérez T, Trumbore SE, Tyler SC, Matson PA, Ortiz-Monasterio I, Rahn T, et al. Identifying the agricultural imprint on the global N_2O budget using stable isotopes. J Geophys Res-Atmospheres. 2001; 106: 9869–9878. doi:10.1029/2000JD900809

32. Pérez T, Trumbore SE, Tyler SC, Davidson EA, Keller M, de Camargo PB. Isotopic variability of N_2O emissions from tropical forest soils. Glob Biogeochem Cycles. 2000; 14: 525–535. doi:10.1029/1999GB001181

33. Peters B, Casciotti KL, Samarkin VA, Madigan MT, Schutte CA, Joye SB. Stable isotope analyses of NO2–, NO3–, and N_2O in the hypersaline ponds and soils of the McMurdo Dry Valleys, Antarctica. Geochim Cosmochim Acta. 2014; 135: 87–101. doi:10.1016/j.gca.2014.03.024

34. Priscu JC, Christner BC, Dore JE, Westley MB, Popp BN, Casciotti KL, et al. Supersaturated N_2O in a perennially ice-covered Antarctic lake: Molecular and stable isotopic evidence for a biogeochemical relict. Limnol Oceanogr. 2008; 53: 2439–2450.

35. Baulch HM, Schiff SL, Thuss SJ, Dillon PJ. Isotopic character of nitrous oxide emitted from streams. Environ Sci Technol. 2011; 45: 4682–4688. doi:10.1021/es104116a PMID: 21534582

36. Rock L, Ellert BH, Mayer B, Norman AL. Isotopic composition of tropospheric and soil N_2O from successive depths of agricultural plots with contrasting crops and nitrogen amendments. J Geophys Res. 2007; 112. doi:10.1029/2006JD008330

37. Samarkin VA, Madigan MT, Bowles MW, Casciotti KL, Priscu JC, McKay CP, et al. Abiotic nitrous oxide emission from the hypersaline Don Juan Pond in Antarctica. Nat Geosci. 2010; 3: 341–344. doi:10.1038/ngeo847

38. Santoro AE, Casciotti KL, Francis CA. Activity, abundance and diversity of nitrifying archaea and bacteria in the central California Current: Nitrification in the central California Current. Environ Microbiol. 2010; 12: 1989–2006. doi:10.1111/j.1462-2920.2010.02205.x PMID: 20345944

39. Sasaki Y, Koba K, Yamamoto M, Makabe A, Ueno Y, Nakagawa M, et al. Biogeochemistry of nitrous oxide in Lake Kizaki, Japan, elucidated by nitrous oxide isotopomer analysis. J Geophys Res. 2011; 116. doi:10.1029/2010JG001589 PMID: 24307747

40. Smemo KA, Ostrom NE, Opdyke MR, Ostrom PH, Bohm S, Robertson GP. Improving process-based estimates of N_2O emissions from soil using temporally extensive chamber techniques and stable isotopes. Nutr Cycl Agroecosystems. 2011; 91: 145–154. doi:10.1007/s10705-011-9452-2

41. Townsend-Small A, Pataki DE, Tseng LY, Tsai C-Y, Rosso D. nitrous oxide emissions from wastewater treatment and water reclamation plants in Southern California. J Environ Qual. 2011; 40: 1542. doi:10.2134/jeq2011.0059 PMID: 21869516

42. Townsend-Small A, Pataki DE, Czimczik CI, Tyler SC. Nitrous oxide emissions and isotopic composition in urban and agricultural systems in Southern California. J Geophys Res. 2011; 116. doi:10.1029/2010JG001494 PMID: 24307747

43. Townsend-Small A, Prokopenko MG, Berelson WM. Nitrous oxide cycling in the water column and sediments of the oxygen minimum zone, eastern subtropical North Pacific, Southern California, and Northern Mexico (23°N-34°N). J Geophys Res Oceans. 2014; 119: 3158–3170. doi:10.1002/2013JC009580

44. Toyoda S, Yoshida N, Urabe T, Aoki S, Nakazawa T, Sugawara S, et al. Fractionation of N_2O isotopomers in the stratosphere. J Geophys Res-Atmospheres. 2001; 106: 7515–7522. doi:10.1029/2000JD900680

45. Toyoda S, Yoshida N, Urabe T, Nakayama Y, Suzuki T, Tsuji K, et al. Temporal and latitudinal distributions of stratospheric N_2O isotopomers. J Geophys Res. 2004; 109. doi:10.1029/2003JD004316

46. Toyoda S, Iwai H, Koba K, Yoshida N. Isotopomeric analysis of N_2O dissolved in a river in the Tokyo metropolitan area. Rapid Commun Mass Spectrom. 2009; 23: 809–821. doi:10.1002/rcm.3945 PMID: 19222057

47. Toyoda S, Yano M, Nishimura S, Akiyama H, Hayakawa A, Koba K, et al. Characterization and production and consumption processes of N_2O emitted from temperate agricultural soils determined via isotopomer ratio analysis. Glob Biogeochem Cycles. 2011; 25, GB2008. doi:10.1029/2009GB003769

48. Tumendelger A, Toyoda S, Yoshida N. Isotopic analysis of N_2O produced in a conventional wastewater treatment system operated under different aeration conditions. Rapid Commun Mass Spectrom. 2014; 28: 1883–1892. doi:10.1002/rcm.6973 PMID: 25088132

49. Van Groenigen JW, Zwart KB, Harris D, van Kessel C. Vertical gradients of $\delta^{15}N$ and $\delta^{18}O$ in soil atmospheric N_2O—temporal dynamics in a sandy soil. Rapid Commun Mass Spectrom. 2005; 19: 1289–1295. doi:10.1002/rcm.1929 PMID: 15838846

50. Well R, Flessa H, Jaradat F, Toyoda S, Yoshida N. Measurement of isotopomer signatures of N_2O in groundwater. J Geophys Res. 2005; 110. doi:10.1029/2005JG000044

51. Well R, Eschenbach W, Flessa H, von der Heide C, Weymann D. Are dual isotope and isotopomer ratios of N_2O useful indicators for N_2O turnover during denitrification in nitrate-contaminated aquifers? Geochim Cosmochim Acta. 2012; 90: 265–282. doi:10.1016/j.gca.2012.04.045

52. Westley MB, Yamagishi H, Popp BN, Yoshida N. Nitrous oxide cycling in the Black Sea inferred from stable isotope and isotopomer distributions. Deep Sea Res Part II. 2006; 53: 1802–1816. doi:10.1016/j.dsr2.2006.03.012

53. Xiong ZQ, Khalil MAK, Xing G, Shearer MJ, Butenhoff C. Isotopic signatures and concentration profiles of nitrous oxide in a rice-based ecosystem during the drained crop-growing season. J Geophys Res. 2009; 114. doi:10.1029/2008JG000827

54. Yamagishi H, Westley MB, Popp BN, Toyoda S, Yoshida N, Watanabe S, et al. Role of nitrification and denitrification on the nitrous oxide cycle in the eastern tropical North Pacific and Gulf of California. J Geophys Res. 2007; 112. doi:10.1029/2006JG000227

55. Yamulki S, Toyoda S, Yoshida N, Veldkamp E, Grant B, Bol R. Diurnal fluxes and the isotopomer ratios of N_2O in a temperate grassland following urine amendment. Rapid Commun Mass Spectrom. 2001; 15: 1263–1269. doi:10.1002/rcm.352 PMID: 11466781

56. Yano M, Toyoda S, Tokida T, Hayashi K, Hasegawa T, Makabe A, et al. Isotopomer analysis of production, consumption and soil-to-atmosphere emission processes of N_2O at the beginning of paddy field irrigation. Soil Biol Biochem. 2014; 70: 66–78. doi:10.1016/j.soilbio.2013.11.026

57. Yoshinari T, Altabet MA, Naqvi SWA, Codispoti L, Jayakumar A, Kuhland M, et al. Nitrogen and oxygen isotopic composition of N_2O from suboxic waters of the eastern tropical North Pacific and the Arabian Sea-Measurement by continuous-flow isotope-ratio monitoring. Mar Chem. 1997; 56: 253–264. doi:10.1016/S0304-4203(96)00073-4

58. Yoshida N, Toyoda S. Constraining the atmospheric N_2O budget from intramolecular site preference in N_2O isotopomers. Nature. 2000; 405: 330–334. doi:10.1038/35012558 PMID: 10830958

59. Zhu R, Liu Y, Li X, Sun J, Xu H, Sun L. Stable isotope natural abundance of nitrous oxide emitted from Antarctic tundra soils: effects of sea animal excrement depositions. Rapid Commun Mass Spectrom. 2008; 22: 3570–3578. doi:10.1002/rcm.3762 PMID: 18932270

60. Zou Y, Hirono Y, Yanai Y, Hattori S, Toyoda S, Yoshida N. Isotopomer analysis of nitrous oxide accumulated in soil cultivated with tea (*Camellia sinensis*) in Shizuoka, central Japan. Soil Biol Biochem. 2014; 77: 276–291. doi:10.1016/j.soilbio.2014.06.016

61. Bauer B, Reynolds M. Recovering data from scanned graphs: Performance of Frantz's g3data software. Behav Res Methods. 2008; 40: 858–868. doi:10.3758/BRM.40.3.858 PMID: 18697681

62. Yang H, Gandhi H, Ostrom NE, Hegg EL. Isotopic fractionation by a fungal P450 nitric oxide reductase during the production of N_2O. Environ Sci Technol. 2014; 48: 10707–10715. doi:10.1021/es501912d PMID: 25121461

63. Jackson AL, Inger R, Parnell AC, Bearhop S. Comparing isotopic niche widths among and within communities: SIBER—Stable Isotope Bayesian Ellipses in R: Bayesian isotopic niche metrics. J Anim Ecol. 2011; 80: 595–602. doi:10.1111/j.1365-2656.2011.01806.x PMID: 21401589

64. Batschelet E. Circular Statistics in Biology. London: Academic Press; 1981.

65. Toyoda S, Suzuki Y, Hattori S, Yamada K, Fujii A, Yoshida N, et al. Isotopomer analysis of production and consumption mechanisms of N_2O and CH_4 in an advanced wastewater treatment system. Environ Sci Technol. 2011; 45: 917–922. doi:10.1021/es102985u PMID: 21171662

66. Kool DM, Wrage N, Oenema O, Harris D, Van Groenigen JW. The 18O signature of biogenic nitrous oxide is determined by O exchange with water. Rapid Commun Mass Spectrom. 2009; 23: 104–108. doi:10.1002/rcm.3859 PMID: 19061209

67. Snider DM, Venkiteswaran JJ, Schiff SL, Spoelstra J. Deciphering the oxygen isotope composition of nitrous oxide produced by nitrification. Glob Change Biol. 2012; 18: 356–370. doi:10.1111/j.1365-2486.2011.02547.x

68. Snider DM, Venkiteswaran JJ, Schiff SL, Spoelstra J. A new mechanistic model of $\delta^{18}O$- N_2O formation by denitrification. Geochim Cosmochim Acta. 2013; 112: 102–115. doi:10.1016/j.gca.2013.03.003

69. Mohn J, Wolf B, Toyoda S, Lin C-T, Liang M-C, Brüggemann N, et al. Interlaboratory assessment of nitrous oxide isotopomer analysis by isotope ratio mass spectrometry and laser spectroscopy: current status and perspectives. Rapid Commun Mass Spectrom. 2014; 28: 1995–2007. doi:10.1002/rcm.6982 PMID: 25132300

70. Thuss SJ, Venkiteswaran JJ, Schiff SL. Proper interpretation of dissolved nitrous oxide isotopes, production pathways, and emissions requires a modelling approach. PLoS ONE. 2014; 9: e90641. doi:10.1371/journal.pone.0090641 PMID: 24608915

71. Ogawa M, Yoshida N. Intramolecular distribution of stable nitrogen and oxygen isotopes of nitrous oxide emitted during coal combustion. Chemosphere. 2005; 61: 877–887. doi:10.1016/j.chemosphere.2005.04.096 PMID: 15993467

72. Toyoda S, Yamamoto S, Arai S, Nara H, Yoshida N, Kashiwakura K, et al. Isotopomeric characterization of N_2O produced, consumed, and emitted by automobiles. Rapid Commun Mass Spectrom. 2008; 22: 603–612. doi:10.1002/rcm.3400 PMID: 18247408

73. Ogawa M, Yoshida N. Nitrous oxide emission from the burning of agricultural residue. Atmos Environ. 2005; 39: 3421–3429. doi:10.1016/j.atmosenv.2005.01.059 PMID: 15952345

74. Prather MJ, Holmes CD, Hsu J. Reactive greenhouse gas scenarios: Systematic exploration of uncertainties and the role of atmospheric chemistry. Geophys Res Lett. 2012; 39, L09803. doi:10.1029/2012GL051440

75. Stock BC, Semmens BX. MixSIAR GUI User Manual, version 2.1.2. 2013. Available: https://github.com/brianstock/MixSIAR.

76. Parnell AC, Inger R, Bearhop S, Jackson AL. Source partitioning using stable isotopes: coping with too much variation. PLoS ONE. 2010; 5: e9672. doi:10.1371/journal.pone.0009672 PMID: 20300637